31st Annual International Conference of the IEEE EMBS
Minneapolis, Minnesota, USA, September 2-6, 2009

Combined Photoacoustic and Magneto-Acoustic Imaging

Min Qu, Srivalleesha Mallidi, Mohammad Mehrmohammadi, Li Leo Ma,
Keith P. Johnston, Konstantin Sokolov, and Stanislav Emelianov, *Member, IEEE*

Abstract— **Ultrasound is a widely used modality with excellent spatial resolution, low cost, portability, reliability and safety. In clinical practice and in the biomedical field, molecular ultrasound-based imaging techniques are desired to visualize tissue pathologies, such as cancer. In this paper, we present an advanced imaging technique – combined photoacoustic and magneto-acoustic imaging – capable of visualizing the anatomical, functional and biomechanical properties of tissues or organs. The experiments to test the combined imaging technique were performed using dual, nanoparticle-based contrast agents that exhibit the desired optical and magnetic properties. The results of our study demonstrate the feasibility of the combined photoacoustic and magneto-acoustic imaging that takes the advantages of each imaging techniques and provides high sensitivity, reliable contrast and good penetrating depth. Therefore, the developed imaging technique can be used in wide range of biomedical and clinical application.**

I. Introduction

Imaging techniques including X-ray computed tomography (CT), ultrasound (US) imaging and magnetic resonance imaging (MRI) are valuable tools for early detection of pathologies such as cancer. Among all the modalities, ultrasound-based imaging techniques are widely used in various medical fields because of their excellent resolution, portability and low cost. In addition, ultrasound imaging is non-ionizing and has no known adverse bioeffects [1]. Ultrasound imaging can be used to obtain an anatomical map of the tissues or organs. However, there are some limitations in the detection effectiveness of pathologies using ultrasound imaging due to its contrast mechanism [1]. Recently, various ultrasound-based techniques such as magneto-motive ultrasound (MMUS) imaging [2-4] and photoacoustic imaging [5-7] have been developed. Combined with ultrasound, MMUS and photoacoustic imaging can be used to obtain molecular images and to provide biomechanical and functional information with respect to an anatomical map of the tissues [1].

In MMUS, magnetic excitation is applied to induce motion of the magnetic nanoparticles within tissues or organs. The moving nanoparticles taken by the tissue can be detected and imaged using ultrasound [2-4]. Therefore, tissue motion is indicative of the presence and concentration of magnetic nanoparticles. Furthermore, the mechanical properties of the magnetically labeled tissue can be evaluated based on an analysis of tissue motion that is detected during MMUS imaging. Therefore, the pathological changes in tissue, which are often related to changes in tissue mechanical properties, could be detected and differentiated using this imaging technique. Consequently, MMUS imaging may be an effective tool to provide real-time assessment of physiological uptake and accumulation of magnetic nanoparticles in tissue and then biomechanical information of the tissue. The contrast in MMUS imaging is determined by the presence and concentration of magnetic particles and is independent of ultrasound imaging. However, the sensitivity of the MMUS imaging technique is limited by the magnetic susceptibility of the magnetic nanoparticles and the induced motion of the tissue containing nanoparticles.

Photoacoustic imaging [5-7] is based on optical absorption of pulsed laser light and subsequent generation of acoustic waves. The contrast mechanism in photoacoustic imaging is related to optical absorption which, in turn, is related to tissue function and composition [1]. The photoacoustic technique exploits both high contrast associated with optical imaging techniques and the spatial resolution of ultrasound imaging. Metal nanoparticles of various shapes and sizes, including gold or silver nanospheres, nanorods and nanoshells can be used as photoabsorbers [8-11]. By varying the shape and aspect ratio of nanoparticles [11], photoacoustic imaging can be performed at the desired wavelength across a wide range of the optical spectrum [12-15].

Both MMUS and photoacoustic imaging provide valuable functional information to detect tissue pathologies. However, the shortcomings of MMUS and photoacoustic imaging limit the impact of these techniques. In this paper, we present the feasibility of combined ultrasound,

Manuscript received April 23, 2009. This work was supported in part by the National Institutes of Health under grants EB 008821 and EB 008101.

Min Qu and Srivalleesha Mallidi are equal contributors.

Corresponding author: Stanislav Emelianov is an Associate Professor in the Department of Biomedical Engineering, University of Texas at Austin (1 University Station C0800, BME 4.202L, Austin, TX 78712-0238, phone: 512-471-1733; fax: 512-471-0616; e-mail: emelian@mail.utexas.edu).

Min Qu, Srivalleesha Mallidi and Mohammad Mehrmohammadi are with the Ultrasound Imaging and Therapeutics Research Laboratory in the Department of Biomedical Engineering, University of Texas at Austin, Austin, TX 78712 (e-mail: M. Qu: qumin@mail.utexas.edu; S. Mallidi: valleesha@austin.utexas.edu, M. Mehrmohammadi: mehrmohammadi@mail.utexas.edu).

Keith P. Johnston is a Professor in the Department of Chemical Engineering, University of Texas at Austin (1 University Station C0400, Austin, TX 78712, e-mail: kpj@che.utexas.edu).

Konstantin Sokolov is an Associate Professor in the Imaging Physics Department at the University of Texas M.D. Anderson Cancer Center, Houston, TX 77030 (e-mail: konstantin.sokolov@engr.utexas.edu).

Leo Ma is in the Department of Chemical Engineering, University of Texas at Austin (e-mail: leoma@mail.utexas.edu).

photoacoustic and magneto-acoustic imaging to simultaneously assess anatomical, functional and biomechanical properties of pathologies such as cancer. The combined imaging takes full advantage of all three modalities and may provide reliable contrast and high sensitivity at a reasonable penetrating depth. The combined imaging method can be used in broad range of applications ranging from fundamental research to biomedical and clinical studies. For example, ultrasound, photoacoustic and magneto-acoustic imaging can be applied to guide photothermal therapy and monitor the outcome [15, 16].

II. Materials and Methods

A. Tissue-mimicking samples

The mixture of 5 nm iron oxide nanoparticles (Fe_3O_4) and 20 nm gold (Au) nanospheres were used as optical and magnetic agent. The Fe_3O_4 nanoparticles and Au nanospheres were custom-made [2, 3, 9]. Briefly, Fe_3O_4 particles were synthesized by coprecipitation of Fe2+ and Fe3+ ions in alkaline conditions with a modification of a method described previously [17], while the Au particles were synthesized via citrate reduction of HAuCl4 under reflux [13].

The experiments were performed using tissue-mimicking samples [2, 3, 9] made out of 10% polyvinyl alcohol (PVA) mixed with nanoparticles. The concentration of Fe_3O_4 nanoparticles in samples was 0.5 mg/mL, and the concentration of Au nanospheres was approximately 10^{11} particles/mL. In addition, 0.5% concentration of 30 µm size silica particles was added to all samples to act as ultrasound scatterers.

B. Imaging system

A block diagram and a photograph of the experimental setup for the combined ultrasound, photoacoustic and magneto-acoustic imaging are shown in Figure 1.

The samples were placed in a water cuvette attached to a 3-D positioning stage. A Q-switched Nd:YAG laser (532 nm wavelength, 5 ns pulse duration, 10 Hz pulse repetition frequency) was used to generate photoacoustic transients. The light was delivered through seven 600 µm diameter optical fibers, as shown in Figure 1. The pulsed magnetic field was produced by a magnetic pulser (model MP5, Sota Instruments, Inc.) connected to a focused magnetic coil, as shown in Figure 1. The 48 MHz single-element focused ultrasound transducer with a focal depth of 5.8 mm was used to obtain ultrasound, photoacoustic and magneto-acoustic images of the samples. The focal points of the optical fibers, the magnetic coil and the ultrasound transducer were aligned. The imaging system consists of a microprocessor unit with a custom-built LabVIEW application that controls the pulsed magnetic source, laser, data acquisition unit, and motion axes for mechanical scanning [9, 13]. The 2-D ultrasound, photoacoustic and magneto-acoustic images were obtained by mechanically scanning the water cuvette over the desired region with 25 µm lateral steps.

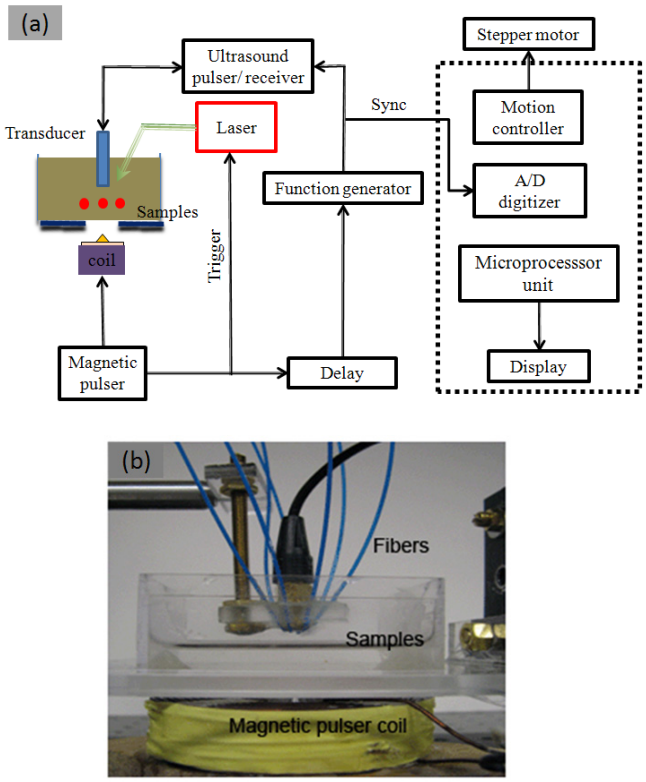

Fig. 1. (a) Block diagram of experimental setup for combined ultrasound, photoacoustic and magneto-acoustic imaging. (b) Photograph of the integrated imaging probe consisting of 48 MHz single-element ultrasound transducer surrounded by optical fibers for uniform laser light irradiation. The magnetic field is applied using magnetic coil located underneath the water cuvette with imaged samples.

In the imaging experiment, the output trigger signal from the magnetic pulser was used as the master trigger because the duration and pulse repetition frequency of magnetic pulses were determined by the internal electronic circuitry of the pulser. The master trigger was produced 20 ms before the magnetic pulse, and photoacoustic imaging was performed during this delay period, as shown in Figure 2. In addition, ultrasound imaging was performed both before and after the magnetic pulse interrogated the tissue.

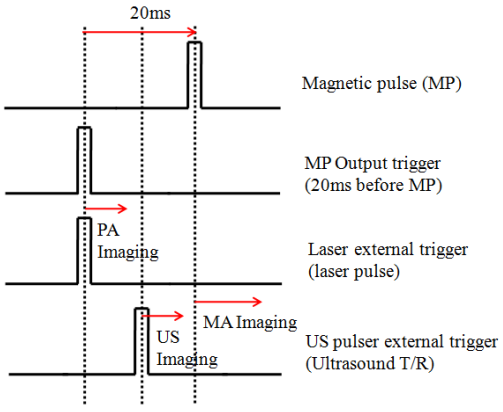

Fig. 2. Schematic representation of the imaging sequence.

The photoacoustic pressure waves, detected by an ultrasound transducer, were used to form the photoacoustic image. The ultrasound signals from the sample were

obtained right after the photoacoustic image. Then a pulsed magnetic field (with duration of about 10 ms) excited the magnetic nanoparticles to induce the motion within the sample. The ultrasound-based image of magnetically induced motion was formed using the signals captured by the same ultrasound transducer. Therefore, the photoacoustic, ultrasound and magneto-acoustic images of the same cross-section were obtained.

III. Results and Discussion

The ultrasound (US), magneto-acoustic (MA) and photoacoustic (PA) images of the samples with Fe_3O_4 nanoparticles and Au nanospheres are shown in Figure 3. The control PVA sample without nanoparticles was used as control. To compare the results, the control sample, the sample with Au nanospheres and Fe_3O_4 nanoparticles, the sample with Au nanospheres only and the sample with Fe_3O_4 nanoparticles only were imaged under the same conditions.

All samples can be clearly observed in the ultrasound image as shown in Figure 3a. However, the control PVA sample is not well visible in magneto-acoustic (Figure 3b) or photoacoustic (Figure 3c) images due to the lack of magnetic and optical contrast agents. The sample with Au nanospheres generates an approximately 200-mV photoacoustic signal. This is expected since gold nanoparticles are used as contrast agents in photoacoustic imaging. However, this sample exhibits almost no contrast in the magneto-acoustic image. The sample with Fe_3O_4 nanoparticles – contrast agents for magneto-acoustic imaging, generates around 150-μm displacement in the pulsed magnetic field. This sample can also be seen in the photoacoustic image because of the elevated optical absorption of a high concentration of Fe_3O_4 nanoparticles. Importantly, the sample with a mixture of Fe_3O_4 nanoparticles and Au nanospheres exhibits the contrast in both photoacoustic and magneto-acoustic images.

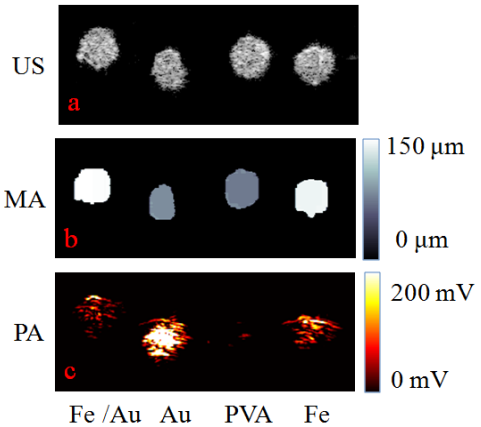

Fig. 3. (a) Ultrasound (US), (b) magneto-acoustic (MA) and (c) photoacoustic (PA) images of the samples containing (left to right) mixture of Fe_3O_4 nanoparticles and Au nanospheres, Au nanospheres only, PVA only (no nanoparticles), and Fe_3O_4 nanoparticles only. All images cover 7.5 mm by 3.0 mm area.

In the magneto-acoustic image, the motion of inclusions in the pulsed magnetic field was detected by the ultrasound waves and the biggest displacement of each pixel in the inclusion was used to build the image. The background motion for the control sample was 5 to 10 μm. The motion for sample with Au nanospheres was almost the same as background motion of the control sample.

Figure 4 shows the extinction spectrum for the solutions of Fe_3O_4 nanoparticles, Au nanospheres and the mixture of both. For Au nanosphere solution, as expected, the spectrum has peak absorption around the 532 nm, which is the wavelength used in our experiments. The extinction for Fe_3O_4 nanoparticle solution at this wavelength is very high primarily due to scattering although there is a finite optical absorption. Indeed, the sample with Fe_3O_4 nanoparticles produces photoacoustic signal – the magnitude of the photoacoustic transients is proportional to the optical absorption coefficient. As shown in Figure 4, the extinction for the solution of the mixture of Fe_3O_4 and Au nanoparticles is a little higher than the solution of Fe_3O_4 itself in the wavelength range of 600-800 nm. It is because the concentration of Fe_3O_4 nanoparticles used in the experiment is almost 10 times higher than that of Au spheres. As the proportion of Fe_3O_4 increases, the extinction of the solution would increase.

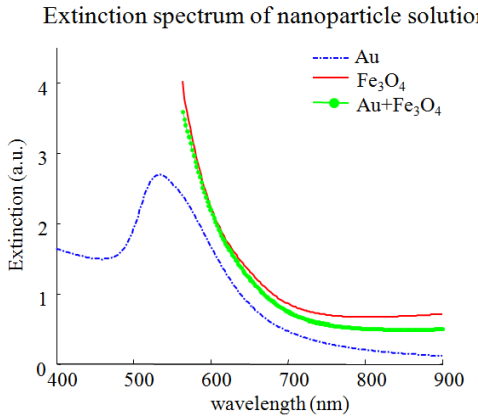

Fig. 4. Extinction spectrum for Fe_3O_4 nanoparticles, Au nanospheres and mixture of both.

To achieve reasonable penetration in tissue and to increase the contrast, near infrared (NIR) wavelength laser light should be used in photoacoustic imaging. Indeed, blood is a strong optical absorber in the 500-600 nm range while water absorbs highly beyond 1300 nm. Therefore, to demonstrate the applicability of combined ultrasound, photoacoustic and magneto-acoustic imaging for biomedical applications, the imaging experiments were performed using the mixture of Fe_3O_4 nanoparticles and Au nanorods (Au*). Gold nanorods can be designed and fabricated to reach characteristic peak absorption in NIR region [11]. A tunable OPO laser system operating at 800 nm wavelength was used to match the optical absorption peak of the Au nanorods. The PVA samples mixed with Fe_3O_4 nanoparticles and Au nanorods showed good contrast in 800 nm photoacoustic image and magneto-acoustic image. Because of high concentration of Fe_3O_4 nanoparticles in the sample, it also

generated photoacoustic signal.

Our results clearly indicate that combined ultrasound, photoacoustic and magneto-acoustic imaging can be used to detect the magnetic and optical nanoparticles with reliable sensitivity and contrast. This imaging technique provides functional and morphological information for the tissues and organs, which could be applied to differentiate abnormal tissues from surrounding normal tissues and to detect pathologies such as cancer in the early stage. In addition, the combined ultrasound, photoacoustic and magneto-acoustic imaging technique can be used both to guide and to enhance photothermal therapy [15, 16, 18, 19].

In the current study, magnetic nanoparticles were directly mixed with plasmonic nanoparticles to form a dual (magnetic and photoacoustic) contrast agent. The experiment results demonstrated the feasibility of combined photoacoustic and magneto-acoustic imaging. Therefore, in the future the hybrid, dual-imaging nanoparticles will be designed with improved magnetic properties. For example, carbon-coated cobalt nanoparticles or dumbbell Au/Fe nanoparticles [20] will be explored in future studies.

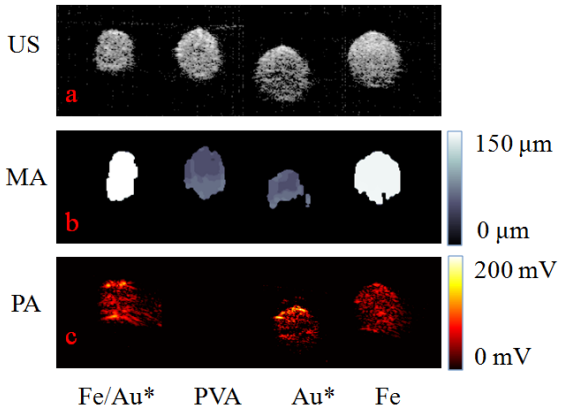

Fig. 5. (a) Ultrasound (US), (b) magneto-acoustic (MA) and (c) photoacoustic (PA) images of the samples containing (left to right) mixture of Fe_3O_4 nanoparticles and Au nanorods, PVA only (no nanoparticles), Au nanorods only, and Fe_3O_4 nanoparticles only. The images cover 8.00 mm by 2.35 mm area.

IV. Conclusion

The combined photoacoustic and magnetic-acoustic imaging uses both optical and magnetic properties as contrast agents to simultaneously assess anatomical, functional and biomechanical properties of pathologies such as cancer. The combined imaging has reasonable contrast, spatial/temporal resolution and sensitivity. As an effective, non-invasive, non-ionizing imaging technique, the combined imaging method can be used in a broad range of clinical and biomedical applications.

References

[1] S. Y. Emelianov, S. R. Aglyamov, A. B. Karpiouk, S. Mallidi, S. Park, S. Sethuraman, J. Shah, R. W. Smalling, J. M. Rubin, and W. G. Scott, "Synergy and applications of combined ultrasound, elasticity, and photoacoustic imaging," *Proceedings of the 2006 IEEE Ultrasonics Symposium*, pp. 405-415, 2006.

[2] M. Mehrmohammadi, J. Oh, L. Ma, S. Roo, E. Yantsen, S. Mallidi, K. P. Johnston, K. Sokolov, T. E. Milner, and S. Y. Emelianov, "Pulsed magneto-motive ultrasound imaging," *Abstract of the 25th Annual Houston Conference on Biomedical Engineering Research, The Houston Society for Engineering in Medicine and Biology*, p. 75, 2008.

[3] M. Mehrmohammadi, L. M. J. Oh, E. Yantsen, T. Larson, S. Mallidi, S. Park, K. P. Johnston, K. Sokolov, T. Milner, and S. Emelianov, "Imaging of iron oxide nanoparticles using magneto-motive ultrasound," *Proceedings of the 2007 IEEE Ultrasonics Symposium*, pp. 652 - 655, 2007.

[4] J. Oh, M. D. Feldman, J. Kim, C. Condit, S. Emelianov, and T. E. Milner, "Detection of magnetic nanoparticles in tissue using magneto-motive ultrasound," *Nanotechnology*, vol. 17, pp. 4183-4190, 2006.

[5] M. H. Xu and L. H. V. Wang, "Photoacoustic imaging in biomedicine," *Review of scientific instruments*, vol. 77, pp. 041101-1 - 041101-22, 2006.

[6] R. A. Kruger, "Photoacoustic ultrasound," *Med. Phys.*, vol. 21, pp. 127-131, 1994.

[7] A. A.Oraevsky, S. L.Jacques, R. O. Esenaliev, and F. K. Tittel, "Laser-based optoacoustic imaging in biological tissues," *Proc. SPIE,* vol. 2134A, pp. 122-128, 1994.

[8] P. C. Li, C. W. Wei, C. K. Liao, C. D. Chen, K. C. Pao, C. R. C. Wang, Y. N. Wu, and D. B. Shieh, "Multiple targeting in photoacoustic imaging using bioconjugated gold nanorods," *Photons Plus Ultrasound: Imaging and Sensing 2006: The 7th Conference on Biomedical Thermoacoustics, Optoacoustics, and Acousto-optics, Proc. of SPIE*, vol. 6086, p. 60860M, 2006.

[9] S. Mallidi, T. Larson, J. Aaron, K. Sokolov, and S. Emelianov, "Molecular specific optoacoustic imaging with plasmonic nanoparticles," *Optics Express*, vol. 15, pp. 6583-6588, 2007.

[10] K. Homan, S. Gomez, H. Gensler, J. Shah, L. Brannon-Peppas, and S. Emelianov, "Design and development of multifunctional contrast agents for photoacoustic imaging," *Proc. of SPIE*, vol. 7190, pp. 71900I-1-71900I-7, 2009.

[11] S. Link and M. A. E. Sayed, "Spectral properties and relaxation dynamics of surface plasmon electronic oscillations in gold and silver nanodots and nanorods," *J. Phys. Chem. B*, vol. 103, pp. 8410-8426, 1999.

[12] X. Yang, S. E. Skrabalak, Y. X. Z. Y. Li, and L. V. Wang, "hotoacoustic Tomography of a rat cerebral cortex in vivo with Au nanocages as optical contrast agent," *Nano Lett.*, vol. 7, pp. 3798-3802, 2007.

[13] E. Y. S. Mallidi, T. Larson, K. Sokolov, and S. Emelianov, "Molecular specific photoacoustic imaging with plasmonic nanosensors," *Proc. of SPIE* vol. 6856, pp. 685616-2, 2008.

[14] J. A. Copland, M. Eghtedari, V. L. Popov, N. Kotov, N. Mamedova, M. O. Motamedi, and A. A. Oraevsky, "Bioconjugated gold nanoparticles as a molecular based contrast agent: implications for imaging of deep tumors using optoacoustic tomography," *Mol. Imaging Biol*, vol. 6, 2004.

[15] C. Loo, A. Lin, L. Hirsch, M. H. Lee, J. Barton, N. Halas, J. West, and R. Drezek, "Nanoshell-enabled photonics-based imaging and therapy of cancer," *Technol Cancer Res Treat*, vol. 3, pp. 33-40, 2004.

[16] J. Kim, S. Park, J. E. Lee, S. M. Jin, J. H. Lee, I. S. Lee, I. Yang, J. S. Kim, S. K. Kim, M. H. Cho, and T. Hyeon, "Designed fabrication of multifunctional magnetic gold nanoshells and their application to magnetic resonance imaging and photothermal therapy," *Angew. Chem. Int. Ed.*, vol. 45, pp. 7754-7758, 2006.

[17] T. Shen, R. Weissleder, M. Papisov, A. Bogdanov, and T. J. Brady, "Monocrystalline iron-oxide nanocompounds (MION) - physicochemical properties," *Magnetic Resonance in Medicine*, vol. 29, pp. 599-604, 1993.

[18] J. Shah, S. Thomsen, T. E. Milner, and S. Y. Emelianov, "Ultrasound guidance and monitoring of laser-based fat removal," *Lasers Surg Med.*, vol. 40, pp. 680-687, 2008.

[19] J. Shah, S. Park, S. Aglyamov, T. Larson, L. Ma, K. Sokolov, K. Johnston, T. Milner, and S. Y. Emelianov, "Photoacoustic imaging and temperature measurement for photothermal cancer therapy," *Journal of Biomedical Optics*, vol. 13, pp. 034024-1 - 034024-9, 2008.

[20] H. Yu, M. Chen, P. M. Rice, S. X. Wang, R. L. White, and S. Sun, "Dumbbell-like bifunctional Au-Fe3O4 nanoparticles," *Nano Lett.*, vol. 5, pp. 379-382, 2005.